Comparative Evaluation of Occupancy Grid Mapping Methods Using Sonar Sensors*

João Carvalho and Rodrigo Ventura

Institute for Systems and Robotics,
Instituto Superior Técnico - Technical University of Lisbon,
Lisbon, Portugal,
{jcarvalho, rodrigo.ventura}@isr.ist.utl.pt

Abstract. Building occupancy grid maps with sonar sensors is a challenging task due to angular uncertainty, specular reflections and crosstalk. This paper presents a quantitative comparison of two probabilistic and one heuristic approaches to the robotic mapping using real sonar data – inverse and forward sensor models and the CEMAL methods. Moreover, the two probabilistic methods are also tested pre-filtering the sonar data with the CEsp filter, which is part of the CEMAL approach. The results show that, using the pre-filtering, all algorithms present a similar and better performance, while without filtering the inverse method presents the highest error.

1 Introduction

One commonly used map representation in robotics is the *occupancy grid map* (OccGrid map), which aims to geometrically represent the environment through a grid discretization of the space. To gather information about the robot environment, one frequently used sensor is the sonar. Sonars are cheap and allow the construction of maps even with a low number of sensors. Despite these advantages, sonars suffer from *angular uncertainty*, *specular reflections* and *crosstalk* between each other, causing erroneous and conflicting measurements [3].

OccGrid mapping was first introduced by Elfes and Moravec in 1985, making use of *inverse sensor models* (ISM) [5]. In this approach, cells are assumed conditionally independent given the robot poses and measurements. In 2001, Thrun proposed an alternative approach using *forward sensor models* (FSM) [6]. This method approaches the mapping problem in the high-dimensional space of all binary maps, trying to solve erroneous and conflicting sonar measurements which affect the ISM results. Recently, Lee and Chung proposed the Conflict-Evaluated Maximum Approximated Likelihood (CEMAL), which is an heuristic method that includes sonar data filtering with the CEsp filter[4].

This paper aims at quantitatively comparing these three OccGrid mapping methods using real sonar data. The impact of the CEsp filter in the ISM and FSM results is also assessed. Due to unclear literature, and in order to produce

* This work was supported by project the FCT [PEst-OE/EEI/LA0009/2011].

meaningful results, the FSM is subject to changes with respect to the original formulation.

2 OccGrid Maps with Inverse Sensor Models

In this approach, the mapping problem is treated inversely to how sonar data is generated, being formulated as

$$p(M|z_{1:T}, x_{1:T}), \tag{1}$$

where M represents the complete map, $z_{1:T}$ represents the complete set of measurements and $x_{1:T}$ are the corresponding poses. This is the denominated *inverse sensor model*.

To simplify the mapping problem, it is assumed that the occupancy of the cells is conditionally independent given measurements and the robot trajectory, transforming the mapping problem into a binary estimation problem,

$$p(M|z_{1:T}, x_{1:T}) = \prod_i p(m_i|z_{1:T}, x_{1:T}), \tag{2}$$

where m_i is an individual cell of the complete map. Other assumption made is the *static world* assumption, considering a measurement t conditionally independent from the previous measurements given the map knowledge. This is a common assumption in mapping but given the decomposition into a binary problem this becomes a much stronger and also incorrect assumption, since it considers conditional independence given only a map cell and not the complete map. This binary estimation problem can be tackled with a binary Bayes filter with static state, parameterized with log-odds:

$$l_i^t = \log \frac{p(m_i|z_t, x_t)}{1 - p(m_i|z_t, x_t)} - \log \frac{p(m_i)}{1 - p(m_i)} + l_i^{t-1}, \tag{3}$$

where l_i^t represents $\log \frac{p(m_i|z_{1:t}, x_{1:t})}{1-p(m_i|z_{1:t}, x_{1:t})}$. The term l_i^{t-1} equals $\log \frac{p(m_i)}{1-p(m_i)}$ when $t = 1$. The probability $p(m_i)$ is the prior of occupancy of the cell i of the map. A typical and simple approach is to model the posterior $p(m_i|z_t, x_t)$ not as a fixed functional form but by a finite number of values which roughly approximate the posterior [3]. For the cells at distances between 0 and the neighbourhood of the measurement the occupancy probability has a low value, in the neighbourhood it has a high value and 0.5 beyond.

Making use of (3) the log-odds occupancy representation can be easily computed for each cell that falls into the coverage cone of the sonar measurements.The desired occupancy probability of the cells can be recovered through

$$p(m_i|z_{1:t}, x_{1:t}) = 1 - \frac{1}{1 + e^{l_i^t}}, \tag{4}$$

resulting in a map of occupancy beliefs for each individual cell.

3 OccGrid Maps with Forward Sensor Models

This approach deals with the mapping problem in its complete state space and assumes the world is static. It uses *forward sensor models*, modelling the mapping as a maximum likelihood estimation problem:

$$p(z_{1:T}|M, x_{1:T}). \tag{5}$$

The goal is to maximize (5), by iteratively adjusting M till no better model is found.

Rather than assuming that all measurements are caused by an obstacle, three possible cases of beam reflection are considered, *maximum reading*, *random* and *non-random*. A non-random measurement is caused by an obstacle in the sonar beam. A maximum value reading happens with the failure in detecting all the obstacles, when present, and returning the maximum range value, z_{max}. The random case models the remaining causes, such as specular reflections.

For the measurement with index t, consider K_t to be the number of obstacles present in the sonar cone, $d_{t,k}$ the distance from the k'th obstacle in the cone and D_t the set of obstacle distances in ascending order. Consider the binary variables $c_{t,*}$, $c_{t,k}$, $c_{t,0}$, which are equal to 1 when the measurement is random, caused by obstacle k or equal to the maximum range, respectively. For each t, only one can be equal to 1.

The random case is modeled as a uniform distribution in the entire sonar range, since the reading could have been caused in any part of the sonar cone. When the beam is reflected by an obstacle, it is considered that it is affected by additive white gaussian noise. In the case where $z_t = z_{max}$, since it is a discrete event, a Dirac delta function is considered. The sensor model can be written as the combination of each of these models:

$$p\left(z_t|M, x_t, c_t\right) = p\left(z_t|M, x_t, c_{t,*} = 1\right)^{c_{t,*}} \prod_{k=0}^{K_t} p\left(z_t|M, x_t, c_{t,k} = 1\right)^{c_{t,k}}. \tag{6}$$

One can now define the prior probability of the causes as

$$p\left(c_t|M, x_t\right) = p\left(c_{t,*} = 1|M, x_t\right)^{c_{t,*}} \prod_{k=0}^{K_t} p\left(c_{t,k} = 1|M, x_t\right)^{c_{t,k}} \tag{7}$$

$$p\left(c_t|M, x_t\right) = \begin{cases} p_{rand} & \text{if } c_{t,*} = 1, \\ p_{max} & \text{if } c_{t,0} = 1, K_t \geq 1, \\ \left(1 - p_{rand} - p_{max}\right) \prod_{i=1}^{k-1} \left[\left(1 - p_{hit}^{(i)}\right)\right] p_{hit}^{(k)} & \text{if } c_{t,k} = 1, k \geq 1, \end{cases} \tag{8}$$

where p_{rand} is the prior probability of a measurement being random, p_{max} is the prior probability of a measurement being maximum and $p_{hit}^{(i)}$ is the prior of the obstacle i to reflect the sonar beam. The p_{hit} probability is function of the obstacle's width coverage in the sonar cone, varying linearly between a minimum and a maximum value and being equal to the maximum value when the obstacle covers 100% of the cone width. Therefore, an obstacle might be formed by one

or more occupied cells, forming a *cluster*. Cells are clustered having as criterium its distance to the sonar cone origin. A cluster is initially formed by a single cell in which further cells are added if the difference between its distance, $d_{t,k}$, and the cluster center of mass is smaller then a given threshold. When a cell does not meet this criterium, a new cluster is created with it.

One can use (6) and (7) and define the log-likelihood of the complete set of measurements with the correspondence variables as the latent variables, compute the expected likelihood over those variables and use the Expectation-Maximization (EM) algorithm to maximize the resulting likelihood [1]. Therefore, the *expected log-likelihood* to maximize is given by:

$$\begin{aligned} & E\left[\log p\left(z_{1:T}, c_{1:T} | M, x_{1:T}\right) | z_{1:T}, x_{1:T}, M\right] \\ & = E\left\{\sum_{t}^{T} \log p\left(z_t | M, x_t, c_t\right) p\left(c_t | M, x_t\right) | z_{1:T}, x_{1:T}, M\right\}. \end{aligned} \tag{9}$$

On the original formulation, the event of a maximum measurement is a particular case of the non-random case. As proposed in this paper, considering the maximum reading event as a different event of the non-random case and defining $p(z_t|M, x_t, c_{t,0} = 1)$ as a Delta dirac function makes those readings have no influence in the likelihood and in the process of maximization, contrary to what happens in the original formulation. Making p_{hit} function of the coverage and the introduction of clustering allows the representation of the angular uncertainty, which is a process not clear in [6].

On the maximization process with the EM, no terms are discarded in (9), since any change in M might produce significant value variations in those terms. To find the map M that maximizes the likelihood, the occupancy of the cells that fall into the measurements cone is flipped and maintained if its new value increases the likelihood value. The maximization process stops when no flipping increases the likelihood. Given the discretization made, this results in a very greedy algorithm, in which the final result highly depends on the cell flipping order. Since it gave empirically good results, in this implementation we chose to first flip the cells closest to the measurement and progressively moving away. The Dirac delta function in $p\left(z_t|M, x_t, c_{t,k} = 1\right)$ is implemented as a gaussian distribution with a very low variance.

4 CEMAL

Sonar sensor readings are characterized by two regions: occupied and empty. The occupied region is the region of occupied cells within a certain neighbourhood of the measurement. The empty region is the region of unoccupied cells between the sonar cone origin and the measurement neighbourhood. For time t, the occupied and empty regions are represented by $O(t)$ and $E(t)$, respectively.

Inconsistencies occur when multiple measurements overlap. Uncertain regions, $U(t)$, are inconsistent regions where a partial part of the occupancy region of a measurement is overlapped with empty regions of other measurements, Figure 1(a). A conflict region, $F(t)$, is an inconsistent region where the complete

occupied region of a measurement is overlapped with empty regions of other measurements, Figure 1(b). [4]

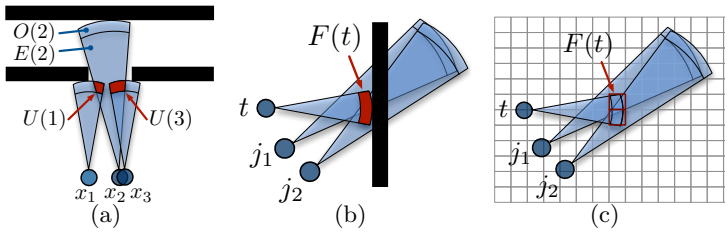

Fig. 1. Inconsistent and conflict cells: (a) uncertain cells, $U(t)$; (b) conflict cells, $F(t)$; (c) discretized conflict cells $F(t)$.

The candidates to incorrect measurements are the measurements causing conflict regions, such as the measurements Figure 1(b) presents. To recognize the incorrect measurements between the candidates the Conflict Evaluation with sound pressure (CEsp) filter is used.

4.1 CEsp

The CEsp method is a filtering method based on the comparison of the sound pressure of the waves received by the conflicting measurements. The sound pressure of a wave received in a sonar can be represented as

$$\begin{aligned} SP_R(r,\theta) &= c_2 SP_T(2r,0) 10^{\frac{D_T(\theta)}{20}} 10^{\frac{D_R(\theta)}{20}} \\ &= \frac{c_1}{r} 10^{\frac{D_T(\theta)+D_R(\theta)}{20}}, \end{aligned} \tag{10}$$

where r is the distance from the cone origin to the obstacle, θ is the angle of the obstacle relative to the measurement cone heading, D_T and D_R are the transmitting and receiving directivity, respectively, and c_1 is an unknown constant which is canceled when sound pressure levels are compared. For further information on the deduction of (10), consult [4].

Using (10), one can identify the incorrect measurements within the candidates. Figure 1(c) illustrates the conflict cells on a OccGrid map. Consider the measurement that indicates occupancy in the conflicting area as being a positive measurement, P, and the ones that indicate empty space in that area as being negative measurements, N. Consider the hypothesis that a cell in the conflict region is occupied. Comparing the sound pressures of these conflicting measurements, one can conclude about that hypothesis:

- $SP_P \geq SP_N$: If there is an obstacle in the conflict cell, the negative reading might miss it, since its sound pressure is lower the sound pressure from the positive reading. Thereby, it is considered that the obstacle exists;

- $SP_P < SP_N$: If there is an obstacle in the conflict cell, the negative measurement cannot miss it, as its sound pressure is higher than the pressure of the positive one. Hence, it is considered that there is no obstacle present.

For instance, for the example of Figure 1(c), consider that it is revealed, through the just described comparison method, that there is an obstacle in any of the conflict cells. Then, since the obstacle is in their empty region, it is considered that measurements j_1 and j_2 are incorrect and must be discarded.

This filtering method is used to ensure that incorrect measurements are discarded and no conflict regions exist, remaining only consistent and uncertain regions.

4.2 Maximum Approximated Likelihood

In the MAL method, it is assumed that the incorrect measurements were discarded by the CEsp filtering. Therefore, and given that sonar sensors were designed to provide the distance to the closest obstacle in their perceiving cone, it is considered that a reliable OccGrid map can be built through

$$\arg\max_M p(z_{1:T}|M, x_{1:T}) = \arg\min_M \sum_t (z_t - d(N_t))^2, \tag{11}$$

where M is the map, $z_{1:T}$ and $x_{1:T}$ are the set of measurements and corresponding poses, z_t is the measurement in time instante t and $d(N_t)$ is the distance from the sonar cone origin to its nearest obstacle N_t. It is made the assumption that a measurement z_t is conditionally independent from the previous measurements given the map M and the robot path.

It is considered that the error is minimized when $|z_t - d(N_t)| \leq \beta$, where β is the range uncertainty. Thereby, it is considered that the global solution to (11) can be found when N_t is placed in the occupied region of the measurement. Therefore, the mapping problem is reduced to a simple problem: cells in uncertain regions are set to unoccupied and the remaining cells in occupied regions are set to occupied.

5 Results

The robot used was the Pioneer P3-AT, equipped with eight SensComp 600 Series sonar sensors and a Sick LMS200 laser rangefinder. Both the ground truth map and the robot pose estimates were obtained using the laser rangefinder and the *GMapping* method [2]. The measurements were taken with the robot moving approximately at $0.6m/s$ and measurements being taken with a $4Hz$ frequency on a single lap to the environment. Two variations of the ISM approach were implemented. The first is as described in section 2 but removing the maximum range measurements, in which specular reflections often result, and in the second it was given less weight to larger measurements. The ISM and FSM methods were also tested with the CEsp pre-filtering.

The ground truth map is presented on Figure 2(a), overlapped with the path made by the robot while the it was acquiring sonar data. Figure 2(b) presents the cones of the sonar measurements. The red/clearer cones are the ones the CEsp filtering discarded. The maps resulting from the implemented algorithms are presented in remaining items of Figure 2.

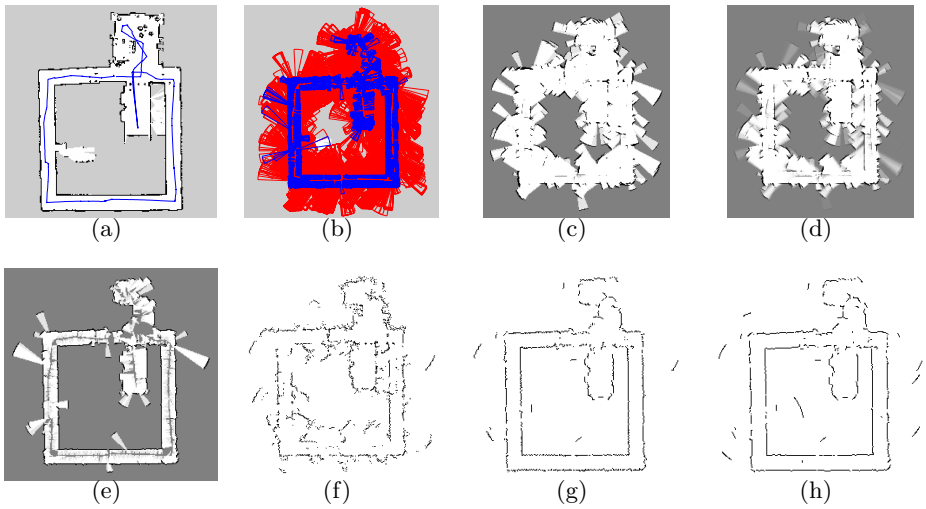

Fig. 2. Results: (a) ground truth map and robot path; (b) sonar measurements – red/clearer measurements are the ones discarded by CEsp; (c) ISM map; (d) ISM with measurement decay map; (e) ISM with CEsp map; (f) FSM map; (g) FSM with CEsp map; (h) CEMAL map.

To compare the results, one computed for each algorithm the overall errors (OE) and the true positive rates (TPR) and false positive rates (FPR). The OE is the percentage of incorrectly classified cells. The TPR is the ratio of the number of occupied cells correctly classified cells over the occupied cells in the ground truth, while FPR is the rate of the number of cells incorrectly classified as unoccupied over the unoccupied cells in the ground truth map. The overall error for each dataset is presented in Figure 3(a). Figure 3(b) shows a plot of the ROC space in which one is able to present the TPR and FPR. From OE, one can conclude that, without filtering, the FSM presents better map than the ISM. All the methods including filtering present a similar error, which is about half of the errors without filtering. Through the ROC, one can see that the methods with filtering represent more of the obstacles present in the ground truth, with the ISM plus CEsp presenting the best TPR. Moreover, with filtering, results do not present as many ghost obstacles.[1]

[1] Additional datasets and corresponding results can be accessed in *www.isr.ist.utl.pt/~jcarvalho.*

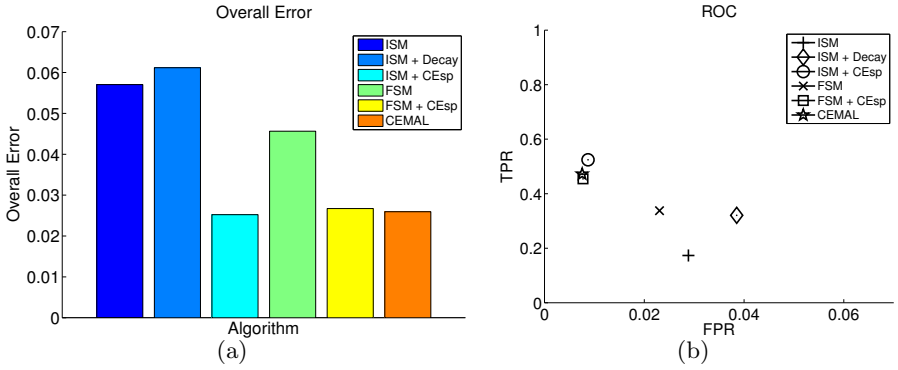

Fig. 3. Comparison metrics results: (a) overall error for each dataset; (b) ROC graphic.

6 Conclusion

This paper presented a comparison between OccGrid mapping using ISM, FSM and the CEMAL methods, with the CEsp filtering also being tested with the first approaches. The results showed that the CEsp filtering as a significant impact on the final map produced by the methods. With filtering, the FSM presents lower error. Future work consists in presenting statistically significant results using multiple datasets and in studying better approaches using forward sensor models, to achieve better results without filtering.

References

1. A.P. Dempster, N.M. Laird, and D.B. Rubin, *Maximum likelihood from incomplete data via the EM algorithm.* Journal of the Royal Statistical Society. Series B (Methodological), pages 138, 1977.
2. G.Grisetti, C.Stachniss, andW.Burgard, *Improvedtechniquesfor grid mapping with rao-blackwellized particle filters.* Robotics, IEEE Transactions on, 23(1):3446, 2007.
3. S. Thrun, W. Burgard, and D. Fox, *Probabilistic Robotics.* MIT Press, ISBN 0262201623, 2005.
4. K. Lee, J.S. Lee, C. Kim, and W.K. Chung, *Effective maximum likelihood grid map with conflict evaluation filter using sonar sensors.* Robotics and Automation, 2009. ICRA09. IEEE International Conference on, pages 16231630. IEEE, 2009.
5. H. Moravec and A. Elfes. High resolution maps from wide angle sonar. In *Robotics and Automation. Proceedings. 1985 IEEE International Conference on*, volume 2, pages 116–121. IEEE, 1985.
6. S. Thrun. Learning occupancy grids with forward models. In *Intelligent Robots and Systems, 2001. Proceedings. 2001 IEEE/RSJ International Conference on*, volume 3, pages 1676–1681. IEEE, 2001.